Channelrhodopsin-mediated optogenetics highlights a central role of depolarization-dependent plant proton pumps

Antonella Reyer[a,1], Melanie Häßler[a,1], Sönke Scherzer[a], Shouguang Huang[a], Jesper Torbøl Pedersen[b], Khaled A. S. Al-Rasheid[c], Ernst Bamberg[d], Michael Palmgren[b], Ingo Dreyer[e], Georg Nagel[a,2], Rainer Hedrich[a,3], and Dirk Becker[a,3]

[a]Institute for Molecular Plant Physiology and Biophysics, University of Würzburg, D-97082 Würzburg, Germany; [b]Department of Plant and Environmental Sciences, University of Copenhagen, DK-1871 Frederiksberg C, Denmark; [c]Zoology Department, College of Science, King Saud University, 11451 Riyadh, Saudi Arabia; [d]Department of Biophysical Chemistry, Max Planck Institute of Biophysics, D-60438, Frankfurt am Main, Germany; and [e]Center of Bioinformatics, Simulation and Modeling, Faculty of Engineering, Universidad de Talca, 3460000 Talca, Chile

Edited by Natasha V. Raikhel, Center for Plant Cell Biology, Riverside, CA, and approved July 2, 2020 (received for review March 25, 2020)

In plants, environmental stressors trigger plasma membrane depolarizations. Being electrically interconnected via plasmodesmata, proper functional dissection of electrical signaling by electrophysiology is basically impossible. The green alga *Chlamydomonas reinhardtii* evolved blue light-excited channelrhodopsins (ChR1, 2) to navigate. When expressed in excitable nerve and muscle cells, ChRs can be used to control the membrane potential via illumination. In *Arabidopsis* plants, we used the algal ChR2-light switches as tools to stimulate plasmodesmata-interconnected photosynthetic cell networks by blue light and monitor the subsequent plasma membrane electrical responses. Blue-dependent stimulations of ChR2 expressing mesophyll cells, resting around −160 to −180 mV, reproducibly depolarized the membrane potential by 95 mV on average. Following excitation, mesophyll cells recovered their prestimulus potential not without transiently passing a hyperpolarization state. By combining optogenetics with voltage-sensing microelectrodes, we demonstrate that plant plasma membrane AHA-type H^+-ATPase governs the gross repolarization process. AHA2 protein biochemistry and functional expression analysis in *Xenopus* oocytes indicates that the capacity of this H^+ pump to recharge the membrane potential is rooted in its voltage- and pH-dependent functional anatomy. Thus, ChR2 optogenetics appears well suited to noninvasively expose plant cells to signal specific depolarization signatures. From the responses we learn about the molecular processes, plants employ to channel stress-associated membrane excitations into physiological responses.

Arabidopsis | optogenetics | electrical signaling | PM H^+-ATPase

Biological membranes serve as selectivity filters and energy stores. Excitable cells from all living creatures, including plants, employ ionic gradients across their plasma membrane to generate electrical signals in response to sensory input (1–3). To study electrical signaling, electrophysiological techniques, such as patch-clamp, provide for precise experimental control of membrane potential and excitability on isolated animal and plant cells (4). Thereby, it has been shown that ion channels, carriers, and pumps govern the voltage-dependent properties of, for example, guard cells—naturally isolated from the rest of leaf and any kind of plant cell protoplasts—enzymatically disconnected from neighboring cells in a tissue (5).

In intact plant tissues, such as roots or leaves, physical constraints imposed by mechanical and osmotic stress, as well as thermal and light fluctuations, evoke transient membrane depolarizations (6–10). In these tissues, however, all cells are electrically interconnected via plasmodesmata, which form an electrical network. As a consequence, control of membrane potential and excitability via electrophysiology (voltage-clamp) is impossible.

The green alga *Chlamydomonas reinhardtii* navigates by sensing light intensity via the retinal-containing, plasma membrane cation channel channelrhodopsin-2 (ChR2; refs. 11 and 12). Due to its fast activation by light, ChR2 has become an important optogenetic tool in neurobiology to predepolarize and excite nerve cells in a light stimulus-dependent manner (13–15). Here, we designed and established a ChR2-based optogenetic approach in plants and used light to voltage-activate interconnected photosynthetic leaf cells. By expressing light-gated ChR2 in all leaf cells, we were able to simultaneously excite selected leaf areas. Depending on light intensity and period, we depolarized a given cell ensemble in a stepwise manner and studied their dose-dependent membrane-limited electrical responses.

Results

Prolonged Blue Light Exposure Evokes Membrane Depolarization of Leaf Cells. In plants, depolarizations in response to physical stresses appear to trigger a transient activation of ion channels, carriers, and pumps. Recovery from the depolarized state, repolarization, was proposed to involve mainly voltage-dependent K^+ channels and plasma membrane H^+ pumps (2, 16–18). To gain insight into membrane repolarization after depolarization, we made use of blue light-activated ChR2 optogenetic tools—channelrhodopsins

Significance

People for centuries are puzzled how living creatures like plants sense their environment. Plants employ electrical signals to communicate a cue-dependent local status between plants cells and organs. As a first response to biotic and abiotic stresses, the membrane potential of plant cells depolarizes. Recovery from the depolarized state, repolarization, was proposed to involve ion channels and pumps. Here, we established channelrhodopsin (ChR2)-based optogenetics in plants and learned that the plant plasma membrane H^+-ATPase represents the major driver of membrane potential repolarization control during plant electrical signaling, rather than voltage-dependent ion channels.

Author contributions: M.P., G.N., R.H., and D.B. designed research; A.R., M.H., S.S., S.H., J.T.P., and I.D. performed research; A.R., M.H., S.S., S.H., J.T.P., I.D., and D.B. analyzed data; and K.A.S.A.-R., E.B., M.P., I.D., G.N., R.H., and D.B. wrote the paper.

The authors declare no competing interest.

This article is a PNAS Direct Submission.

[1]A.R. and M.H. contributed equally to this work.

[2]Present address: Institute Physiology–Neurophysiology, Biocentre, Julius-Maximilians-University, D-97070 Würzburg, Germany.

[3]To whom correspondence may be addressed. Email: hedrich@botanik.uni-wuerzburg.de or dirk.becker@uni-wuerzburg.de.

This article contains supporting information online at https://www.pnas.org/lookup/suppl/doi:10.1073/pnas.2005626117/-/DCSupplemental.

First published August 11, 2020.

(ChRs; ref. 13). Blue light controls plant growth, development, and stomatal movement via activation of the guard cell plasma membrane (PM) H^+-ATPase (19). To serve as ChR-free control, we initially monitored the blue light membrane response of WT leaf cells using sharp intracellular microelectrodes (Fig. 1*A*). Short blue light pulses did not affect the membrane potential of leaf cells resting at about −160 mV. However, when exposed for ≥50 s to blue light, mesophyll cells—in a singular occurrence—depolarized up to −60 mV (Fig. 1*B*, ΔV = 101.2 ± 3.3 mV). At more depolarized membrane potentials, voltage-dependent K^+ efflux channels tend to open and have thus been discussed as possible key players during the repolarization phase (2). To test the possibility that K^+ efflux channels played a role for the repolarization of the membrane, we exposed the K^+ efflux channel mutant *gork1-2* to blue light irradiation. In response to extended blue light stimulation, membrane repolarization of the K^+ efflux channel mutant was indistinguishable from WT in amplitude and kinetics (Fig. 1*C*).

ChR2 Variants Mediate Robust BL-Induced Depolarization in Plant Cells. What about the plasma membrane H^+ pump? To study the impact of the plasma membrane H^+-ATPase on repolarization from membrane depolarization, we transiently expressed ChR2 in the *Nicotiana benthamiana* system. In search of a channelrhodopsin suited to triggering blue light-induced depolarizations, similar to naturally occurring membrane potential depolarizations, we tested WT ChR2 and variants thereof differing with respect to inactivation and deactivation kinetics (20, 21). *Agrobacterium tumefaciens* harboring ChR2 variants fused to YFP were infiltrated into intact leaves of 4- to 5-wk-old plants (*SI Appendix*, Fig. S1). In leaves expressing ChR2 variants with visible plasma membrane localization, such as $ChR2^{C128T}$, $ChR2^{C128A}$, $ChR2^{D156C}$, and $ChR2^{D156A}$, mesophyll cells showed retinal and blue light-dependent membrane potential depolarizations after 15 s of stimulation, characterized by variant-specific differences in regaining the membrane potential resting state (Fig. 2*A* and *SI Appendix*, Table S1). We further concentrated on $ChR2^{D156C}$ as the ChR2 best-suited for studying depolarization-induced membrane electrical responses in the plant system. This mutant, also known as channelrhodopsin-2-XXL (ChR2-XXL; refs. 22 and 23), depolarizes the plasma membrane in a manner similar to naturally occurring depolarization events in terms of amplitude and depolarization speed (1.04 ± 0.04 s; 103 ± 3.4 mV·s^{-1}). Additionally, the prolonged open probability of the ChR2-XXL variant causes a slow repolarization, which is in the range of repolarization processes observed in plants in response to known physiological biotic or abiotic stimuli (8, 24, 25).

Blue Light Triggers Inward, pH-Dependent Currents in ChR2-XXL Expressing Guard Cells. Next, we generated *Arabidopsis thaliana* plants that stably expressed a YFP-tagged version of the ChR2-XXL, under control of the Cauliflower mosaic virus 35S promoter (*SI Appendix*, Fig. S2). Because ChR2 is gated by blue light, plants were grown in long day conditions under a red light regime (*SI Appendix*, *Extended Methods*). Under these conditions, the phenotype of ChR2-XXL transformants were indistinguishable from control plants. To study ChR2-XXL activity on the single-cell level, we performed voltage-clamp recordings in guard cells, which—in contrast to mesophyll cells—are electrically uncoupled from their surrounding neighbors. When clamped to −100 mV using double-barreled microelectrodes, ChR2-XXL–expressing guard cells exhibited instantaneous inward currents in response to 10-s blue light pulses that slowly deactivated upon pulse cessation (Fig. 2*B*) and were absent from guard cells of control plants (Fig. 2*B*). In line with the observation that channelrhodopsins predominantly conduct protons (15, 26), blue light-triggered currents were highest at pH_{ext} 5.0, intermediate at pH_{ext} 6.0, and almost absent at symmetrical pH (7.0; Fig. 2 *C* and *D*). The small currents remaining in the absence of a proton gradient suggest that the contribution of cations other than protons pass CHR2-XXL is marginally only. Taken together, these results demonstrate that the functional expression of ChR2-XXL in planta provides a noninvasive tool to resolve electrical signaling events in *Arabidopsis* plants.

ChR2-XXL Provides for Noninvasive, BL-Controlled Membrane Depolarizations. We next performed membrane potential recordings on leaf mesophyll cells to dissect the unknown molecular players that contribute to membrane potential repolarization (2). Upon microelectrode impalement with leaves of 5- to 7-wk-old ChR2-XXL–expressing plants, membrane potentials in the range of −176 ± 2.4 mV were recorded, which—when illuminated by short 5-s blue light pulses—depolarized reproducibly (Fig. 3*A*). Without retinal addition, leaves expressing ChR2-XXL only depolarized ∼15 mV. After ≥2 h retinal incubation, however, mean depolarization amplitudes (ΔV) of 95 ± 2.3 mV were recorded (Fig. 3*B* and *SI Appendix*, Fig. S3). Responses of different leaves from individual plants were comparable in blue light response amplitudes and kinetics (Fig. 3*C*). In general, during stimulation, depolarization sets in immediately after initiation of

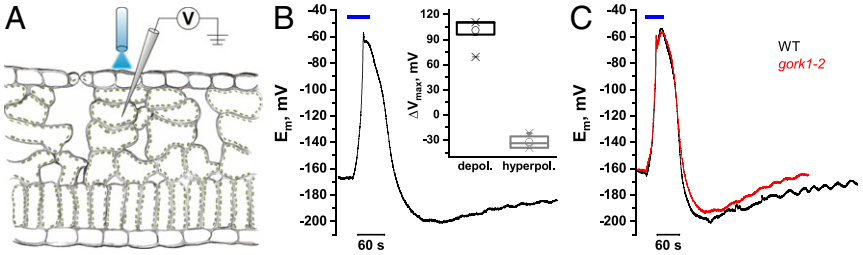

Fig. 1. Blue light induces transient membrane potential depolarizations in *Arabidopsis thaliana* mesophyll cells. (*A*) Diagram showing the experimental setup for recording blue light-induced membrane potential changes in *A. thaliana* mesophyll cells. Note: Leaves were mounted with the adaxial side on the microscope slide and the abaxial epidermis up, facing the bath medium. (*B*) Representative trace of membrane potential recordings using microelectrode impalement of mesophyll cells in intact leaves in response to a 50-s blue light pulse. Upon impalement, typical membrane potentials of ca. −160 to −180 mV were recorded. Upon 50 s of illumination with blue light, fast membrane potential depolarizations to about −60 mV were triggered as a singular event. Membrane potential depolarizations were followed by fast repolarization and transient hyperpolarization, before cells returned to prestimulus membrane potential levels. The mean depolarization (ΔV) triggered by extended blue light pulses was about 101.2 ± 3.3 mV, while the observed hyperpolarization, relative to the recorded resting membrane potential was about −32.5 ± 2.3 mV (*Inset*). (*C*) No difference in kinetics is observed when comparing the blue light-induced depolarization under the same experimental conditions as in *B* between *A. thaliana* WT (Col-0) and the *gork1-2* mutant, indicating that the mesophyll K^+ efflux channel does not contribute to blue light-induced membrane potential changes. External solution was composed of 1 mM KCl, 1 mM $CaCl_2$, 10 mM MES/BTP, pH 6.0. Blue light was applied via fiber optics at an intensity density of 17.5 mW·mm^{-2}.

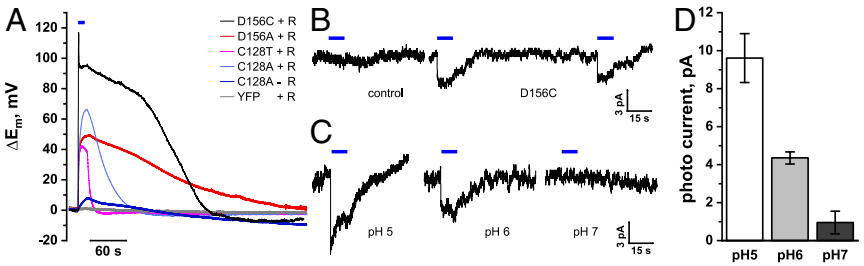

Fig. 2. Blue light activates ChR2-XXL in tobacco mesophyll cells and *Arabidopsis* guard cells. (*A*) Representative voltage traces of blue light-induced depolarization in *N. benthamiana* mesophyll cells expressing YFP (control) or different ChR2 variants. A statistical analysis of the properties of selected ChR2 variants is presented in *SI Appendix*, Table S1 ($n \geq 4$; mean ± SE). Note that blue light did not evoke depolarizations in control cells and that ChR2-mediated depolarizations depended on retinal substitution (*SI Appendix*, Fig. S3). (*B*) Guard cells in isolated epidermal strips were impaled with double-barreled electrodes, filled with 300 mM KOAc (pH 7.0). The plasma membrane potential was clamped at −100 mV and superimposed with a 10-s blue light stimulus. Blue light-stimulated photocurrents were recorded in guard cells expressing ChR2-XXL ($n = 5$) but not in controls (control, $n = 6$). The bath solution was composed of 1 mM KCl, 1 mM $CaCl_2$, and 10 mM MES/BTP, pH 6. (*C* and *D*) External pH affects the ChR2-XXL current. Photocurrents of ChR2-XXL were recorded in guard cells under identical conditions as in *B* but at different pH values as indicated in the figure (mean ± SE, $n \geq 5$).

the blue light pulse and reached peak amplitudes within about 4 s for cells expressing ChR2-XXL. Immediately after stimulus termination, the plant membrane potential repolarized in a biphasic manner toward the prestimulus resting level. Upon extended blue light stimuli longer than 20 s, a transient hyperpolarization following the repolarization phase was frequently observed (Fig. 3*D*). The mean repolarization time—which reflects the time span between peak depolarization and the point of reaching the resting potential—for ChR2-XXL expressing cells was 83 ± 4.5 s, which compares to the reported deactivation time constants of ChR2-XXL expressed in oocytes (22). Considering the pronounced ΔV of almost 100 mV, we calculated the repolarization speed in these cells to -1.2 ± 0.1 mV·s^{-1} (Fig. 3*C*). Starting from a resting potential of about −180 mV, the membrane potential of ChR2-XXL plants instantaneously depolarized to around −80 to −90 mV upon blue light stimulation. The influx of any cation species would be able to depolarize the membrane potential. The relative permeability of ChR2 is, however, about four to six orders of magnitude higher for H^+ compared to other cations, including K^+ or Ca^{2+} (15, 26). To monitor ion fluxes during blue light-activated, ChR2-XXL–mediated membrane potential changes, we thus employed noninvasive scanning ion-selective microelectrodes (SISE) (27, 28). In control experiments, a 5-s blue light stimulation did not affect $[H^+]_{ext}$ (*SI Appendix*, Fig. S4 *A* and *B*). In contrast,

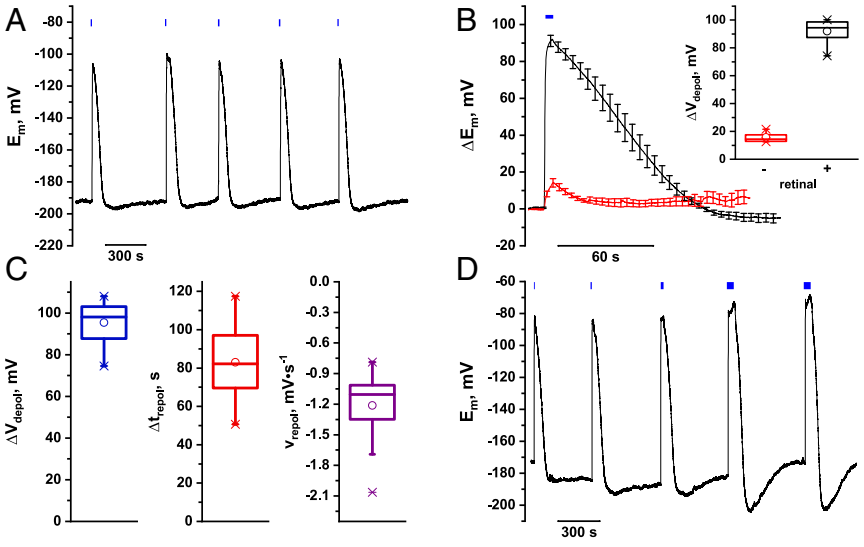

Fig. 3. ChR2-XXL provides for reproducible, blue light-triggered membrane potential depolarizations in *Arabidopsis* mesophyll cells. (*A*) Representative membrane potential recordings in response to 5-s blue light pulses using microelectrode impalement of mesophyll cells in intact *Arabidopsis* leaves expressing ChR2-XXL. Upon impalement, typical membrane potentials of ca. −160 to −190 mV were recorded. Repeated 5-s blue light-pulses triggered fast, reproducible depolarizations of the membrane potential. Depolarizations typically peaked at about −105 mV followed by fast repolarization and weak transient hyperpolarization before cells returned to prestimulus membrane potential levels. (*B*) Mean standardized membrane potential depolarizations of *A. thaliana* mesophyll cells expressing fully reconstituted (100 μM retinal) ChR2-XXL were 92 ± 2.9 mV, ($n = 8$, *Inset*) in response to a 5-s blue light-pulse (black curve). In the absence of retinal, mean depolarizations were only 14 ± 2.4 mV (red curve; $n = 7$, *Inset*). (*C*) Statistic analysis of the standardized membrane potential characteristics from 16 individual plants revealed a mean depolarization of 95 ± 2.3 mV with a minimum of 74 mV, a maximum of 108 mV and a median of 98 mV. Following ChR2-XXL–mediated depolarization, mesophyll cells repolarized toward their resting potential within 83 ± 4.5 s (minimum 51 s, maximum 107 s, and median 82 s). The associated repolarization speed was calculated to -1.2 ± 0.08 mV·s^{-1} (minimum −0.78 mV·s^{-1}, maximum −1.69 mV·s^{-1}, median −1.1 mV·s^{-1}, and an outlier of −2.06 mV·s^{-1}). (*D*) Representative membrane potential recordings of mesophyll cells in intact leaves in response to consecutive, extending blue light pulses (5, 10, 20, 2×50 s). Fast membrane potential depolarizations were observed for each pulse. 50-s blue light pulses, however, caused an additional depolarization (Fig. 1) on top of the ChR2-XXL–based depolarization followed by a pronounced hyperpolarization that was typically absent in response to short, 5-s blue light illumination.

we observed a decrease in $[H^+]_{ext}$ during blue light stimulation in ChR2-XXL–expressing mesophyll cells, corresponding to H^+ influx. When the blue light was switched off, H^+ influx ceased and was followed by H^+ efflux. However, under the same settings, K^+-selective electrodes—despite exhibiting an intrinsic light sensitivity of the K^+-selective mixture—did not display major differences in K^+ fluxes between controls and ChR2-XXL–expressing cells (*SI Appendix*, Fig. S4 *C* and *D*). Together, these findings suggest that, when triggered by blue light, membrane potential depolarization predominantly results from H^+ influx via ChR2-XXL under the given experimental conditions.

Plasma Membrane H^+-ATPase Provides for Major Membrane Repolarizing Activity. The longer the ChR2 gate stays open, the longer the cell is clamped in the depolarizing state and the more protons accumulate at the cytosolic side of the plasma membrane. Further, after blue light stimulation, the membrane potential often transiently hyperpolarizes by approximately −10 mV more negative than the prestimulus level. This overshoot behavior becomes particularly evident when increasing the duration of consecutive stimulations (Fig. 3*D*). Repolarization below E_K, followed by a transient swing to a more hyperpolarized state, can only be explained by the action of a plasma membrane H^+ pump. Thus, in both scenarios, the repolarization kinetics and hyperpolarization amplitude very likely depend on the degree of depolarization and/or H^+ (substrate) activation of the plasma membrane H^+ -ATPase.

To test the H^+ pump hypothesis, we took advantage of vanadate, a potent inhibitor of a large variety of enzymes known to interact with phosphate compounds, including the P-type ATPases (29, 30). Incubation of leaf cells with 1 mM vanadate had a pronounced effect on the prestimulus resting potential and on the biphasic poststimulus repolarization kinetics (Fig. 4 *A* and *C* and *SI Appendix*, Fig. S5*A*). Compared to controls, cells exposed to vanadate exhibited a prolonged repolarization phase (Fig. 4*A* and *SI Appendix*, Fig. S5*B*).

In contrast to inhibitory vanadate, the wilting toxin fusicoccin (FC) represents a potent activator of the proton pump. Fusicoccin locks the PM H^+-ATPase in a phosphorylation-independent active state (31, 32). Application of 4 μM FC to ChR2-XXL–expressing mesophyll cells resulted in hyperpolarization by 26 ± 2 mV within 5 min (*SI Appendix*, Fig. S5*D*). Subsequent blue light-dependent activation of ChR2-XXL resulted in fast membrane potential depolarizations indistinguishable from cells not exposed to FC. However, in the presence of FC, the repolarization phase was significantly accelerated and about 2 times faster when compared to controls (Fig. 4*B* and *SI Appendix*, Fig. S5*E*). Vanadate inhibition and FC stimulation of poststimulus repolarization kinetics and amplitude both supports the notion that the PM H^+-ATPase is predominately responsible for restoring the membrane potential after excitation.

AHA2 Activity Is pH Dependent. Although the cytoplasm is well buffered, the very rapid H^+ influx through ChR2-XXL, triggered by blue light, likely causes substantial pH changes, at least in the immediate vicinity of the plasma membrane. The resulting acidification could change the properties of the PM H^+-ATPase. To study the effects of pH on the PM H^+-ATPase, we expressed the constitutively active mutant aha2Δ92 in the heterologous host *Saccharomyces cerevisiae*, purified the solubilized recombinant protein, and then analyzed the properties of the recombinant pump under the guidance of a theoretical model. Based on the two major conformations, E1 and E2 (33), we translated the mechanistic model of the pump cycle (*SI Appendix*, Fig. S6*A*) into a mathematical description of the pump activity (*SI Appendix*, *Extended Methods*). According to this model, the pump current amplitude is modulated by internal H^+, external H^+, and the membrane voltage. The voltage, at which the pump current is zero, depends on the energy status of the cell (via parameter *A*, Equation A4, *SI Appendix*) and on the transmembrane proton gradient. The fit of the model to the experimental data revealed that the ATP hydrolytic activity of aha2Δ92 increased with cytosolic acidification (pK_i = 7.9) and decreased with extracellular acidification (pKe = 5.9; *SI Appendix*, Fig. S6*B*). In line with this model, decreasing the proton gradient by shifting the extracellular pH from 5.5 to pH 7.5 resulted in an acceleration of repolarization (*SI Appendix*, Fig. S7).

Voltage-Dependent AHA2-Mediated Proton Pumping in *Xenopus* Oocytes Is Fusicoccin and Vanadate Sensitive. Next, we tested our assumption that, in addition to pH_{cyt}, repolarization kinetics and amplitude depend on the degree of depolarization. Although the first primary structure of a plant PM H^+-ATPase and second crystal structures of AHA2 have been known since 1989 and 2007, respectively (33–36), the H^+ pump protein has not yet been characterized electrophysiologically in AHA-free heterologous expression systems (37). To study the voltage-dependent properties of an *Arabidopsis* H^+ pump, in a system unaffected by regulation of the plant cell, we expressed WT AHA2 protein in *Xenopus* oocytes. When the plasma membrane of control oocytes was clamped at −40 mV, reflecting a depolarized plant cell, inward steady-state proton fluxes around 60 $nmol \cdot m^{-2} \cdot s^{-1}$ were measured in SISE experiments by H^+-selective electrodes (Fig. 4*C*) (27, 28). Functional expression of the AHA2-WT protein under these conditions reduced the net H^+ influx by 50%. With the hyperactive aha2Δ73 mutant, which lacks the autoinhibitory C-terminal R domain (38), proton fluxes were reversed and we observed outwardly directed H^+ fluxes (Fig. 4*C*). Upon stepping the membrane toward −210 mV—mimicking a maximally hyperpolarized plant cell—proton pumping vanished (Fig. 4*D*). This demonstrates that the plant PM H^+-pump AHA2 is depolarization-activated. These results were obtained with the aha2Δ73 mutant, which documents that the voltage dependence of the PM H^+-ATPase does not depend on its terminal R domain. Voltage-dependent H^+ pumping in the −40 to −210 mV range was fitted by equation A3 (*SI Appendix*) indicating a half-activation voltage of −140 mV (Fig. 4*D*). Just like in the experiments with *Arabidopsis* mesophyll cells, proton pumping of the oocyte-expressed AHA2 was inhibited by vanadate and stimulated by the fungal toxin FC (Fig. 4*C* and *SI Appendix*, Fig. S8).

Discussion

Microbial opsin-based optogenetics represents a powerful tool to study neuronal networks (39). Although plants employ electrical signaling networks to communicate biotic and abiotic stressors, the application of optogenetics in plants so far has focused on photoreceptor-based interference of gene expression or the manipulation of stomatal aperture via a synthetic blue light-activated K^+ ion channel (40, 41). To study plant electrical signaling, we functionally expressed the opsin ChR2-XXL in *Arabidopsis* leaf cells and identified the plasma membrane H^+-ATPase as the major molecular entity driving recovery from ChR2-XXL–mediated depolarization of the membrane potential (17). According to its intrinsic voltage dependence, the plant PM H^+-ATPase would be activated by blue light-induced, ChR2-XXL–mediated membrane potential depolarizations to rapidly initiate repolarization and return to resting potential levels in *Arabidopsis* mesophyll cells. This is in contrast to animal cells, where the repolarization phase of an action potential is dominated by voltage-dependent K^+ efflux channels (42, 43). In mesophyll cells, however, ChR2-XXL–induced depolarizations do not progress beyond the equilibrium potential for potassium ions (E_K), which would be required to activate voltage-dependent K^+ efflux channels, such as GORK (44). Future studies employing light gated anion channelrhodopsins like ACR1 (45) to depolarize the membrane positive to E_K might provide for additional mechanistic insight into the role of K^+ channels in plant electrical signaling. Given that ChR2-XXL–triggered depolarizations are carried by H^+ influx, local acidic pH deflections might act

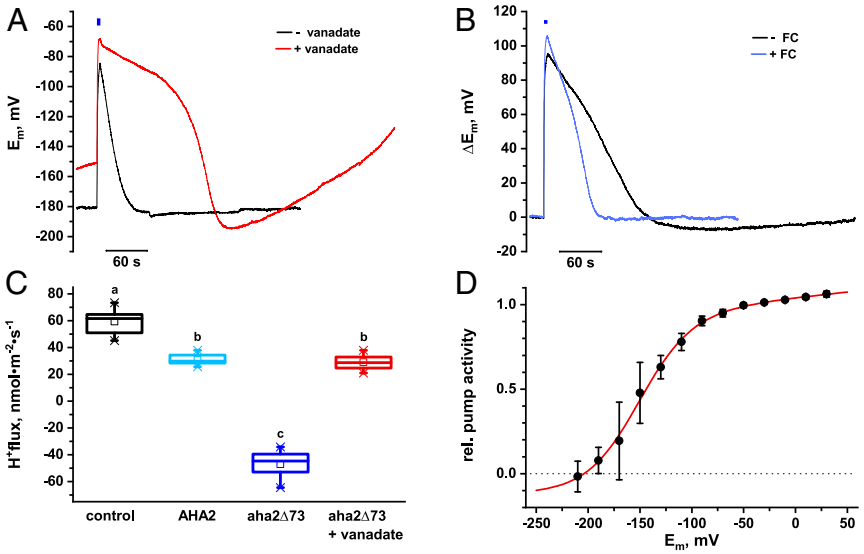

Fig. 4. Proton pump modulators affect repolarization kinetics. (*A*) Representative membrane potential recordings of impaled mesophyll cells preincubated with 1 mM Na_3VO_4 (vanadate, red curve). Traces represent individual depolarizations from a continuous recording cut out and superimposed for comparison. In comparison to control cells (black curve), vanadate inhibition of the PM H^+-ATPase resulted in a positive shift of the prestimulus membrane potential (resting potential, see *SI Appendix*, Fig. S5*C*) and further delayed the repolarization phase by clamping cells in a depolarized state after blue light-induced ChR2-XXL activation. (*B*) The fungal toxin fusicoccin activates the PM H^+-ATPase. Representative membrane potential recordings from ChR2-XXL–expressing mesophyll cells before (black line) and in response to 4 μM fusicoccin (blue line). The repolarization speed of ChR2-XXL–mediated membrane potential transients is significantly accelerated due to hyperstimulated PM H^+-ATPase activity (see also *SI Appendix*, Fig. S6). (*C*) Functional expression of the PM H^+-ATPase in *Xenopus* oocytes. H^+ flux across the *Xenopus* oocyte plasma membrane was measured using the SISE technique. Oocytes were injected with water (black), AtAHA2 WT (light blue), or the aha2Δ73 mutant RNA (blue). After 5 d of expression, oocytes were voltage-clamped to −40 mV and H^+ flux was recorded. Control oocytes exhibited proton influx under tested conditions. Expression of AHA2 WT resulted in significant reduction of net H^+ flux and expression of the constitutively active mutant aha2Δ73 resulted in significant H^+ efflux. Preincubation of aha2Δ73-expressing oocytes for 30 min in 10 mM vanadate resulted in significant reduction of H^+ efflux (red). The bottom and top of the boxes denote the first and third quartiles, respectively, the middle line represents the median, whiskers mark the most extreme values within 1.5 times the interquartile distance below the first or above the third quartile, crosses indicate the first and 99th percentiles, and different letters indicate significantly different values: control-WT, $P = 6.7 \times 10^{-8}$; control-aha2Δ73, $P = 6.7 \times 10^{-8}$; control-aha2Δ73+vanadate, $P = 9.2 \times 10^{-8}$; WT-aha2Δ73, $P = 8.8 \times 10^{-8}$; WT-aha2Δ73+vanadate, $P = 0.4$; aha2Δ73-aha2Δ73+vanadate, $P = 8.7 \times 10^{-8}$; $F_{3,48} = 502.8$, one-way ANOVA, $n \geq 9$ oocytes). (*D*) To determine voltage dependence of H^+-pumping activity, H^+ fluxes were measured in aha2Δ73-expressing oocytes and membrane potential was varied between −210 and +30 mV. Fitting the normalized fluxes with equation (A3; red line) resulted in half-maximal pump activity at −140 mV (mean ± SD, $n \geq 4$).

synergistically with depolarization to trigger activation of the PM H^+-ATPase. Regulation of the PM H^+-ATPase by calcium-dependent networks have been observed (32, 46). Due to the low Ca^{2+} permeability of CHR-XXL, we did not observe activation of Ca^{2+}-dependent anion channels, reported to drive membrane potential depolarizations in response to light, during pathogen recognition or ABA-induced stomatal closure (24, 47–49), but employing highly Ca^{2+}-permeable channelrhodopsins (21, 50) could shed new light on the underlying mechanism. ChR2-XXL—as shown here—provides a valuable tool to study the role of electrogenic transport entities, including PM H^+-ATPases, during electrical signaling of interconnected cells in intact plant tissues. We expect that the broad spectrum of available optogenetic tools (39) will allow the identification and characterization of novel players of—and thus new insights into—plant electrical signaling networks (1, 51).

Materials and Methods

Intracellular Measurements. Before measurements, leaf discs were glued with medical adhesive on coverslips in measurement chambers and incubated in standard bath-solution containing 1 mM KCl, 1 mM $CaCl_2$ and 10 mM 2-(N-morpholino)ethanesulfonic acid (MES), adjusted with Bis-Tris propane to pH 6.0. Leaf discs were allowed to recover overnight in a closed Petri dish in the growth cabinet. Reconstitution of functional ChR2 was achieved by incubation of leaf discs in standard bath solution containing 100 μM all-trans retinal. Before measurements, solution exchange was performed and leaf discs were kept for recovery in the dark (>30 min). For impalement experiments, microelectrodes from borosilicate glass capillaries, with filament (Hilgenberg), were pulled on a horizontal laser puller (P2000, Sutter Instruments). Capillaries were filled with 300 mM KCl and connected via an Ag/AgCl half-cell to a headstage (1 GΩ, HS-2A, Axon Instruments). Tip resistance was about 50 MΩ. The reference electrode was also filled with 300 mM KCl closed with an agarose bridge (2% in 300 mM KCl). A VF 102 Dual Microelectrode amplifier (biologics) was used. The signal was filtered with a LPF202A low-pass Bessel filter (Warner Instruments) and over an AD-converter digitalized. The cells were impaled by an electronic micromanipulator (NC-30, Kleindiek Nanotechnik). Data were analyzed using Origin Pro-2016.

Electrophysiological Recordings on Intact Guard Cells. Epidermal strips were gently peeled with a pair of tweezers and fixed on coverslips. The strips were incubated with a bath solution (0.1 mM KCl, 1 mM $CaCl_2$ and 10 mM MES/bis-tris propane (BTP), pH 6) containing 10 μM retinal at least 2 h, before the start of measurement. The ChR2-XXL–mediated photocurrent was recorded in guard cells with double-barreled borosilicate microelectrodes (Hilgenberg). The double-barreled electrodes were filled with 300 mM KOAc (pH 7.0) and had a tip resistance ranging from 200 to 280 MΩ. Ag/AgCl half-cells were used to connect the electrodes to a custom-made amplifier (Ulliclamp01) equipped with headstages with an input impedance of 1,011 Ω. A reference electrode made from a capillary filled with 300 mM KCl and sealed with 2% agarose was placed in the bath solution. Guard cells were clamped at −100 mV, and currents were recorded in response to 10-s blue light (470 nm) pulses that were supplied by a light-emitting diode (LED)-based optical fiber system (pE-4000, CoolLED). The electrical signals were first low-pass filtered at 0.5 kHz with a dual low-pass Bessel Filter (LPF 202A; Warner Instruments Corp.), and recorded at 1 kHz with the National Instruments interfaces (USB-6002).

ACKNOWLEDGMENTS. We thank members of the AG Nagel—Christoph Stangl and Ronnie Gueta—for initial electrophysiological characterization and dissemination of improved channelrhodopsin mutants as well as Shiqiang Gao for the successful implementation of red light growth

conditions for ChR-XXL transgenes and discussions. We are grateful to Frieda Reisberg (AG Nagel) and Doris Waffler (SFB567) for screening and selecting the Arabidopsis ChR2-XXL lines and Katharina Adam (AG Hedrich) for technical assistance. We thank Frances Sussmilch for critical reading and corrections of the manuscript. This work was supported by grants from the Deutsche Forschungsgemeinschaft (DFG) within the DFG Research Group FOR964 (to D.B. and R.H.) and within the DFG-funded SFB567 Project B10 (to D.B. and G.N.).

1. W. G. Choi, R. Hilleary, S. J. Swanson, S. H. Kim, S. Gilroy, Rapid, long-distance electrical and calcium signaling in plants. *Annu. Rev. Plant Biol.* **67**, 287–307 (2016).
2. R. Hedrich, V. Salvador-Recatalà, I. Dreyer, Electrical wiring and long-distance plant communication. *Trends Plant Sci.* **21**, 376–387 (2016).
3. W. A. Catterall, G. Wisedchaisri, N. Zheng, The chemical basis for electrical signaling. *Nat. Chem. Biol.* **13**, 455–463 (2017).
4. B. Sakmann, E. Neher, *Single-Channel Recording*, (Springer, New York, Dordrecht, Heidelberg, London, ed. 2, 1995).
5. R. Hedrich, J. I. Schroeder, The physiology of ion channels and electrogenic pumps in higher plants. *Annu. Rev. Plant Physiol. Plant Mol. Biol.* **40**, 539–569 (1989).
6. D. Basu, E. S. Haswell, Plant mechanosensitive ion channels: An ocean of possibilities. *Curr. Opin. Plant Biol.* **40**, 43–48 (2017).
7. M. H. Cho, E. P. Spalding, An anion channel in Arabidopsis hypocotyls activated by blue light. *Proc. Natl. Acad. Sci. U.S.A.* **93**, 8134–8138 (1996).
8. J. Fromm, S. Lautner, Electrical signals and their physiological significance in plants. *Plant Cell Environ.* **30**, 249–257 (2007).
9. S. Stoelzle, T. Kagawa, M. Wada, R. Hedrich, P. Dietrich, Blue light activates calcium-permeable channels in Arabidopsis mesophyll cells via the phototropin signaling pathway. *Proc. Natl. Acad. Sci. U.S.A.* **100**, 1456–1461 (2003).
10. F. Yuan *et al*., OSCA1 mediates osmotic-stress-evoked Ca^{2+} increases vital for osmosensing in Arabidopsis. *Nature* **514**, 367–371 (2014).
11. M. Böhm *et al*., Channelrhodopsin-1 phosphorylation changes with phototactic behavior and responds to physiological stimuli in *Chlamydomonas*. *Plant Cell* **31**, 886–910 (2019).
12. O. A. Sineshchekov, K. H. Jung, J. L. Spudich, Two rhodopsins mediate phototaxis to low- and high-intensity light in *Chlamydomonas reinhardtii*. *Proc. Natl. Acad. Sci. U.S.A.* **99**, 8689–8694 (2002).
13. P. Hegemann, G. Nagel, From channelrhodopsins to optogenetics. *EMBO Mol. Med.* **5**, 173–176 (2013).
14. G. Nagel *et al*., Channelrhodopsin-1: A light-gated proton channel in green algae. *Science* **296**, 2395–2398 (2002).
15. G. Nagel *et al*., Channelrhodopsin-2, a directly light-gated cation-selective membrane channel. *Proc. Natl. Acad. Sci. U.S.A.* **100**, 13940–13945 (2003).
16. P. Ache *et al*., GORK, a delayed outward rectifier expressed in guard cells of Arabidopsis thaliana, is a K^+-selective, K^+-sensing ion channel. *FEBS Lett.* **486**, 93–98 (2000).
17. A. Kumari, A. Chételat, C. T. Nguyen, E. E. Farmer, *Arabidopsis* H^+-ATPase AHA1 controls slow wave potential duration and wound-response jasmonate pathway activation. *Proc. Natl. Acad. Sci. U.S.A.* **116**, 20226–20231 (2019).
18. G. Lohse, R. Hedrich, Characterization of the plasma-membrane H^+-ATPase from *Vicia faba* guard cells: Modulation by extracellular factors and seasonal changes. *Planta* **188**, 206–214 (1992).
19. S.-I. Inoue, T. Kinoshita, Blue light regulation of stomatal opening and the plasma membrane H^+-ATPase. *Plant Physiol.* **174**, 531–538 (2017).
20. C. Bamann, R. Gueta, S. Kleinlogel, G. Nagel, E. Bamberg, Structural guidance of the photocycle of channelrhodopsin-2 by an interhelical hydrogen bond. *Biochemistry* **49**, 267–278 (2010).
21. S. Kleinlogel *et al*., Ultra light-sensitive and fast neuronal activation with the Ca^{2+}-permeable channelrhodopsin CatCh. *Nat. Neurosci.* **14**, 513–518 (2011).
22. A. Dawydow *et al*., Channelrhodopsin-2-XXL, a powerful optogenetic tool for low-light applications. *Proc. Natl. Acad. Sci. U.S.A.* **111**, 13972–13977 (2014).
23. F. Scholz, E. Bamberg, C. Bamann, J. Wachtveitl, Tuning the primary reaction of channelrhodopsin-2 by imidazole, pH, and site-specific mutations. *Biophys. J.* **102**, 2649–2657 (2012).
24. E. Jeworutzki *et al*., Early signaling through the Arabidopsis pattern recognition receptors FLS2 and EFR involves Ca-associated opening of plasma membrane anion channels. *Plant J.* **62**, 367–378 (2010).
25. E. Krol *et al*., Perception of the Arabidopsis danger signal peptide 1 involves the pattern recognition receptor AtPEPR1 and its close homologue AtPEPR2. *J. Biol. Chem.* **285**, 13471–13479 (2010).
26. F. Schneider, C. Grimm, P. Hegemann, Biophysics of channelrhodopsin. *Annu. Rev. Biophys.* **44**, 167–186 (2015).
27. J. Dindas *et al*., AUX1-mediated root hair auxin influx governs $SCF^{TIR1/AFB}$-type Ca^{2+} signaling. *Nat. Commun.* **9**, 1174 (2018).
28. S. Scherzer *et al*., Insect haptoelectrical stimulation of Venus flytrap triggers exocytosis in gland cells. *Proc. Natl. Acad. Sci. U.S.A.* **114**, 4822–4827 (2017).
29. J. D. Clausen *et al*., Crystal structure of the vanadate-inhibited Ca^{2+}-ATPase. *Structure* **24**, 617–623 (2016).
30. J. A. Gordon, Use of vanadate as protein-phosphotyrosine phosphatase inhibitor. *Methods Enzymol.* **201**, 477–482 (1991).
31. C. Jelich-Ottmann, E. W. Weiler, C. Oecking, Binding of regulatory 14-3-3 proteins to the C terminus of the plant plasma membrane H^+-ATPpase involves part of its autoinhibitory region. *J. Biol. Chem.* **276**, 39852–39857 (2001).
32. J. Falhof, J. T. Pedersen, A. T. Fuglsang, M. Palmgren, Plasma membrane H^+-ATPase regulation in the center of plant physiology. *Mol. Plant* **9**, 323–337 (2016).
33. D. Focht, T. I. Croll, B. P. Pedersen, P. Nissen, Improved model of proton pump crystal structure obtained by interactive molecular dynamics flexible fitting expands the mechanistic model for proton translocation in P-type ATPases. *Front. Physiol.* **8**, 202 (2017).
34. J. M. Pardo, R. Serrano, Structure of a plasma membrane H^+-ATPase gene from the plant Arabidopsis thaliana. *J. Biol. Chem.* **264**, 8557–8562 (1989).
35. J. F. Harper, T. K. Surowy, M. R. Sussman, Molecular cloning and sequence of cDNA encoding the plasma membrane proton pump (H^+-ATPase) of *Arabidopsis thaliana*. *Proc. Natl. Acad. Sci. U.S.A.* **86**, 1234–1238 (1989).
36. B. P. Pedersen, M. J. Buch-Pedersen, J. P. Morth, M. G. Palmgren, P. Nissen, Crystal structure of the plasma membrane proton pump. *Nature* **450**, 1111–1114 (2007).
37. S. Veshaguri *et al*., Direct observation of proton pumping by a eukaryotic P-type ATPase. *Science* **351**, 1469–1473 (2016).
38. K. B. Axelsen, K. Venema, T. Jahn, L. Baunsgaard, M. G. Palmgren, Molecular dissection of the C-terminal regulatory domain of the plant plasma membrane H^+-ATPase AHA2: Mapping of residues that when altered give rise to an activated enzyme. *Biochemistry* **38**, 7227–7234 (1999).
39. K. Deisseroth, Optogenetics: 10 years of microbial opsins in neuroscience. *Nat. Neurosci.* **18**, 1213–1225 (2015).
40. R. Ochoa-Fernandez *et al*., "Optogenetics in plants: red/far-red light control of gene expression" in *Optogenetics: Methods and Protocols*, A. Kianianmomeni, Ed. (Humana, New York, 2016), pp. 125–139.
41. M. Papanatsiou *et al*., Optogenetic manipulation of stomatal kinetics improves carbon assimilation, water use, and growth. *Science* **363**, 1456–1459 (2019).
42. L. Y. Jan, Y. N. Jan, Voltage-gated potassium channels and the diversity of electrical signalling. *J. Physiol.* **590**, 2591–2599 (2012).
43. A. L. Hodgkin, A. F. Huxley, Currents carried by sodium and potassium ions through the membrane of the giant axon of Loligo. *J. Physiol.* **116**, 449–472 (1952).
44. T. A. Cuin, I. Dreyer, E. Michard, The role of potassium channels in *Arabidopsis thaliana* long distance electrical signalling: AKT2 modulates tissue excitability while GORK shapes action potentials. *Int. J. Mol. Sci.* **19**, 926 (2018).
45. Y. S. Kim *et al*., Crystal structure of the natural anion-conducting channelrhodopsin GtACR1. *Nature* **561**, 343–348 (2018).
46. Y. Yang *et al*., The Ca^{2+} sensor SCaBP3/CBL7 modulates plasma membrane H^+-ATPase activity and promotes Alkali tolerance in Arabidopsis. *Plant Cell* **31**, 1367–1384 (2019).
47. B. D. Lewis, G. Karlin-Neumann, R. W. Davis, E. P. Spalding, Ca^{2+}-activated anion channels and membrane depolarizations induced by blue light and cold in Arabidopsis seedlings. *Plant Physiol.* **114**, 1327–1334 (1997).
48. Y. Liu *et al*., Anion channel SLAH3 is a regulatory target of chitin receptor-associated kinase PBL27 in microbial stomatal closure. *eLife* **8**, e44474 (2019).
49. S. Huang *et al*., Calcium signals in guard cells enhance the efficiency by which abscisic acid triggers stomatal closure. *New Phytol.* **224**, 177–187 (2019).
50. X. Duan, G. Nagel, S. Gao, Mutated channelrhodopsins with increased sodium and calcium permeability. *Appl. Sci.* **9**, 664.2076-3417 (2019).
51. S. A. Mousavi, A. Chauvin, F. Pascaud, S. Kellenberger, E. E. Farmer, GLUTAMATE RECEPTOR-LIKE genes mediate leaf-to-leaf wound signalling. *Nature* **500**, 422–426 (2013).